[American Journal of Science, Vol. 301, April/May, 2001, P. 432–454]

SLOPE DISTRIBUTIONS, THRESHOLD HILLSLOPES, AND STEADY-STATE TOPOGRAPHY

DAVID R. MONTGOMERY

Department of Geological Sciences, University of Washington,
Seattle, Washington 98195

ABSTRACT. Digital elevation models of two "steady-state" mountain ranges, the Olympic Mountains (OM) and Oregon Coast Range (OCR), are used to examine relationships between slope distributions, the development of threshold hillslopes, and steady-state topography. Plots of drainage area versus slope for these mountain ranges exhibit substantial scatter that complicates comparison of range form to analytical theories and landscape evolution models. Contour plots of the density of such data reveal an attractor at the scale of the transition from hillslope processes to channel processes, and log-bin averaging reveals trends that parallel predictions of steady-state erosion laws but with different rate laws for five distinct process domains: hillslopes, valley heads, and colluvial, bedrock, and alluvial valley segments. Slope histograms computed for 100 km^2 areas (defined by a 10 × 10 km grid) throughout the OM exhibit approximately normal or exponential distributions in areas of active rock uplift and depositional topography, respectively. Local slope distributions in the OCR also tend to be normally distributed, but some are left-skewed in areas with gentler slopes. Mean slopes determined both over the above referenced grid and a 10-km diam moving window are relatively invariant in the core of the OM in spite of strong contrasts in bedrock erodibility and gradients in long-term rock uplift rates. In contrast, the mean slopes in the OCR parallel latitudinal gradients in rock uplift rates and bedrock erodibility. Hence, the slope distributions in the OM and OCR reflect distinct relationships between development of threshold bedrock and soil-mantled hillslopes and steady-state topography.

INTRODUCTION

The widespread availability of digital elevation models (DEMs) and of the means to analyze them through increasingly powerful computers and software is revolutionizing the quantitative analysis of landforms. Nowhere is this revolution more apparent than in the resurgence of interest in the interplay of erosion and tectonic processes. In particular, the development and popularization of equations to describe long-term erosion laws, such as the "diffusion law" for hillslope erosion and the family of models now commonly referred to as "stream power laws," have led to the ability to formally model feedback between tectonic forcing, erosion, isostatic rebound, and rock exhumation (Willett, Beaumont, and Fullsack, 1993; Howard, Dietrich, and Seidl, 1994; Montgomery, 1994; Tucker and Slingerland, 1994; Kirkby, 1997; Whipple, Kirby, and Brocklehurst, 1999; Whipple and Tucker, 1999). Such efforts have spawned reexamination of the interaction between the push of tectonic processes and the pull of erosion during the evolution of a mountain range (Beaumont, Fullsack, and Hamilton, 1991; Zeitler, Chamberlain, and Smith, 1993; Koons, 1995; Avouac and Burov, 1996; Norris and Cooper, 1997; Pavlis, Hamburger, and Pavlis, 1997). In addition, the ability to analyze quantitatively whole mountain ranges has both rekindled interest in the related concepts of steady-state topography and threshold hillslopes and revived the integration of hillslope and channel evolution in response to tectonic forcing as a major theme in geomorphology.

As recognized by Davis (1898, 1899), the adjustment of hillslope evolution to river incision is both essential for maintaining steady-state topography and a characteristic that can evolve over the lifetime of a mountain range. Recognition of the predominance of straight hillslopes in some landscapes led to suggestions that slope stability can control hillslope morphology by setting a limiting or threshold slope (Penck, 1924,

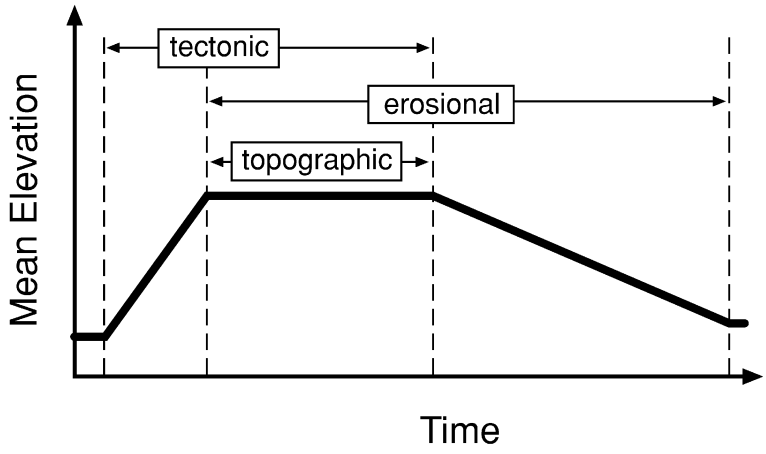

Fig. 1. Illustration of relations between tectonic, erosional, and topographic steady state through the rise and decay of a mountain range. Steady rock uplift rates may record a tectonic steady-state prior to development of an erosional steady state, resulting in net surface uplift. As the topography steepens, erosion rates increase until they balance rock uplift, at which point both a topographic and erosional steady state may be maintained until rock uplift decreases, and the topography declines in mean elevation.

1953). This idea has developed into the concept of a threshold hillslope that maintains a characteristic critical slope while being lowered via landsliding or highly non-linear hillslope sediment transport. The growing recognition of the potentially significant role of threshold hillslopes in the development of steady-state topography motivates the question of how to recognize such features from DEMs. Here I review the development of the concepts of steady-state topography and threshold hillslopes and analyze the DEMs of two steady-state mountain ranges in the western United States to examine relationships between slope distributions, the development of threshold hillslopes, and steady-state topography.

STEADY-STATE TOPOGRAPHY

Several definitions of steady-state can be applied to entire mountain ranges. An erosional steady state characterizes a mountain range in which there are no net sinks or changes in storage of material eroded from the landscape. Such a landscape could be either gaining or losing surface elevation depending upon the relationship between erosion and rock uplift. A tectonic steady-state is one in which the long-term rock uplift rate is constant, but again such a landscape may be gaining or losing surface elevation depending upon the relationship to erosion rates. When both the erosional and tectonic definitions of steady-state are satisfied the resulting topography reflects the steady-state condition of no net change in surface elevation due to a balance between rock uplift and erosion.

These different types of steady state can characterize different periods in the life of an orogen (fig. 1). For a range to rise initially, rock uplift must exceed erosion. Hence, a tectonic steady-state would likely precede a topographic steady state. As long as erosion rates increase along with the mean slope while the range rises, then eventually the erosion rates will balance rock uplift rates. Steady-state topography can then ensue while this balance is maintained. An erosional steady state (as defined above) may persist after tectonic forcing relaxes, rock uplift rates decline, and the topography is lowered, even though erosion rates may slow as mean slopes decline. Hence, steady-state topography occurs only in the phase of mountain building,

wherein erosion rates have equilibrated with rock uplift rates. Consequently, achievement of a topographic steady-state cannot necessarily be inferred independently from either thermochronologic or erosional histories.

The concept of steady-state topography can be traced to the classic works of Gilbert (1877, 1909) and Davis (1898, 1899). Gilbert (1877) recognized that for a landscape eroding everywhere at a uniform rate, and, therefore in an erosional steady state, concave river profiles reflect that a downstream decrease in slope compensates for the greater discharge of larger rivers. Extension of the concept of a uniform lowering rate to the analysis of hillslope form led to the explanation of hilltop convexities as the equilibrium signature of slope-dependent soil transport (Davis, 1892; Gilbert, 1909). By the mid-20th century, Mackin's (1948) elaboration of the concept of the graded river, Strahler's (1950) treatment of the graded drainage system, and Hack's (1960) discussion of landscapes in dynamic equilibrium firmly established the idea that landscape morphology could remain fixed in space if rock uplift balanced erosion. Hence, not only could a landscape erode everywhere at the same rate, but the interplay of uplift and erosion could maintain steady-state topography.

Most erosional processs occur as discrete events—whether by bedrock river incision during an extreme flood, landsliding, the burrowing activity of animals, or the uprooting of trees. Hence, definition of steady-state topography entails implicit or explicit specification of a relevant time frame. In addition, evaluation of steady-state topography requires definition of a spatial scale, as the response time of a hillslope to changes in local boundary conditions or climate forcing (Fernandes and Dietrich, 1997) may be much shorter than the response time for a river system in a large continental drainage basin (Whipple and Tucker, 1999). Development of steady-state topography integrates the coupled response of hillslopes and the channel network over geologic time. Consequently, we need to assess the generalized consequences of many erosional events throughout the evolution of the landscape rather than the dynamics of discrete, stochastic erosional events if we are to address the development of steady state topography in mountain range evolution.

The most general criterion for steady-state topography is that the local erosion rate E everywhere equals the local rock uplift rate U. In general, sediment transport capacity (Q_s) can be described as a function of drainage area (A) and local slope (S):

$$Q_s = KA^mS^n \tag{1}$$

where K is a constant that incorporates climatic factors and erodibility, and m and n are thought to vary with different erosional processes (Kirkby, 1971). Assuming that rock uplift and erosion rates are in balance through an orogen, then the local sediment transport rate must equal the product of the rock uplift rate and the contributing drainage area (Howard, 1994):

$$Q_s = UA \tag{2}$$

For the case of transport-limited erosion, equating eqs. (1) and (2) yields a relationship between drainage area and slope for steady-state topography:

$$S = (U/K)^{(1/n)}A^{(1-m)/n} \tag{3}$$

Note that for the case of detachment-limited channel incision, the erosion rate E is used in the left-hand side of eq (1) which together with the constraint that E = U simplifies the steady-state exponent on drainage area to m/n.

Erosion by hillslope processes is generally characterized as following a "diffusive" transport law wherein m = 0, which would result in a positive relation between drainage area and slope in eq (3). In contrast, fluvial processes are typically considered

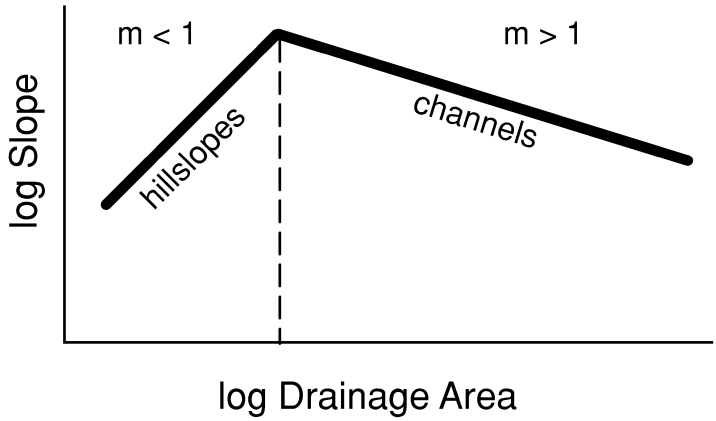

Fig. 2. Relationship between drainage area and slope predicted for steady-state topography under erosional processes described by eq (3).

to have m >1, in which case eq (3) predicts an inverse relationship between drainage area and local slope. Hence, for steady state topography, one would expect to find two relatively simple modes of drainage area-slope scaling expressed across a landscape (fig. 2). Tarboton, Bras, and Rodriguez-Iturbe (1992) identified such a change from a positive to an inverse relationship between drainage area and slope based on averaged trends extracted from 30-m grid DEMs.

Willgoose (1994) constructed a general landscape evolution model based on coupling a channel transport formulation of eq (1) with a slope-dependent, or diffusive, transport law for hillslopes. He found that under conditions of steady-state topography with a constant rock uplift rate, the simulated channel network exhibited the predicted relation between drainage area and slope. In contrast, he also found that under the case of a catchment with no rock uplift and therefore declining relief, the relation between drainage area and slope was less well defined, with each tributary channel exhibiting distinct but highly variable relationships that resulted in substantial scatter to the drainage area-slope relationship for the catchment as a whole. Willgoose's simulations suggest that plots of drainage area versus local slope would constitute a simple test for steady-state topography. A transition from a positive to a well-defined inverse power law relation between drainage area and slope would be expected to characterize a steady-state landscape. In contrast, much greater scatter and different exponents for different tributary basins would be expected to characterize non-steady-state landscapes.

In real landscapes, however, the expression of well-defined power law relations between drainage area and slope are complicated by a number of factors. Debris flow processes in mountain drainage basins can contribute to erosion of headwater valley systems and impart a kink to drainage area-slope relationships (Seidl and Dietrich, 1992; Montgomery and Foufoula-Georgiou, 1993). Threshold-driven or strongly nonlinear hillslope transport rates (Howard, 1994; Roering, Kirchner, and Dietrich, 1999) can impose an upper limit to the slope angles attained in a landscape. In addition, spatial heterogeneity in erosivity also influences landscape-scale relationships between drainage area and slope (Moglen and Bras, 1995). At present, most workers analyze general trends in drainage area versus slope plots by imposing some form of log-bin averaging on DEM-derived data (Tarboton, Bras, and Rodriguez-Iturbe, 1992). But given the variability apparent in and the range of potential influences on drainage

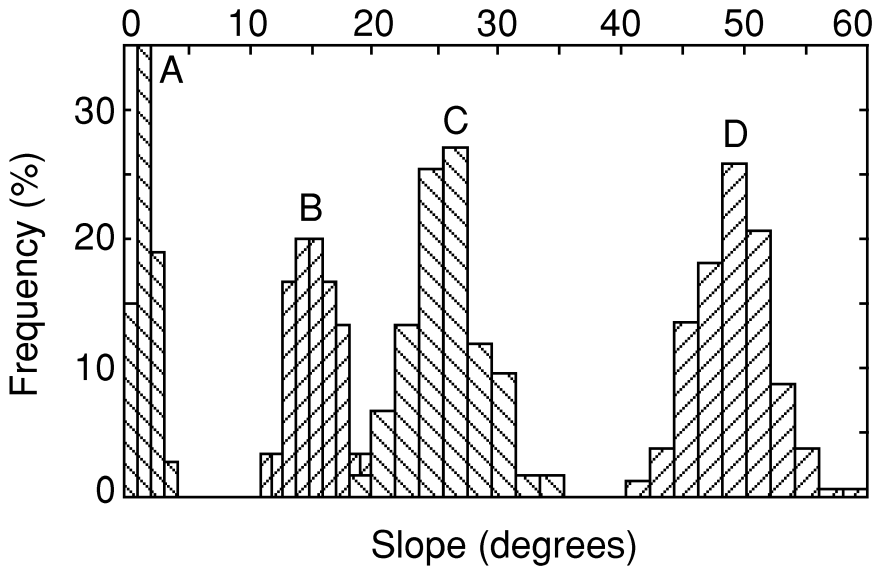

Fig. 3. Histograms of slope frequency distributions for valley side slopes reported by Strahler (1950): (A) Steenvoorde, France, (B) Rose Well gravels, Arizona, (C) Santa Fe Formation, Bernalillo, New Mexico, (D) dissected clay fill, Perth Amboy, New Jersey. Modified from Strahler (1950).

area-slope relationships, the degree to which one can actually assess steady-state from plots of drainage area versus slope remains unclear.

THRESHOLD HILLSLOPES

As for the concept of "steady-state," several distinct definitions of threshold hillslopes have been used in the geomorphological literature. The classic use of the concept has applied primarily to slope stability in soil-mantled landscapes, where regolith properties are argued to set the maximum achievable or threshold slope. A more recent application is to the case of bedrock threshold hillslopes, which were long thought not to be strength limited because of the high cohesion and strength of intact rock. While both soil-mantled and bedrock slopes may be threshold hillslopes, these two types of slopes have different implications for landscape evolution and the development of steady-state topography.

Soil-mantled threshold hillslopes.—Strahler (1950, 1956) ushered in the quantitative analysis of relations between hillslope processes and slope form with his field surveys of valley wall slopes. He showed that the steepest segments of valley walls had normal slope distributions with small standard deviations for a number of areas with widely differing lithology, soil, relief, vegetation, and climate. The mean slopes for the different areas he analyzed ranged from 2° to 49° (fig. 3), and he concluded that hillslopes tended to approach an equilibrium angle (Strahler, 1950). Strahler summarized his findings in his Law of Constancy of Slopes:

> Within an area of essentially uniform lithology, soils, vegetation, climate and stage of development, maximum slope angles tend to be normally distributed with low dispersion about a mean value determined by the combined factors of drainage density, relief and slope-profile curvature (Strahler, 1950, p. 685).

As a result of his analysis Strahler (1950) recognized several types of "graded," or equilibrium slopes: (1) high-cohesion slopes, (2) repose slopes, and (3) slopes reduced by wash and creep. The first category of slopes are those where cohesive soils, strong bedrock, and vegetation can maintain slopes at angles greater than the angle of

internal friction (ϕ) of the slope forming material. In contrast, repose slopes are composed of loose, cohesionless debris, and hillslope angles are therefore controlled by the friction angle of the slope-forming material. Strahler envisioned the third category of slopes, which he considered to be those gentler than about 20°, as shaped by wash and creep and not maintained by active channel incision at their base. Strahler (1950) essentially argued that hillslope angles adjust to reflect rates of channel incision at their base and that the specific slope angles in a landscape reflect a suite of environmental properties.

Young (1961) proposed that slope angles be measured at standard lengths along slope profiles rather than at the steepest point of the valley wall. He argued that peaks in the resulting slope distributions defined "characteristic angles" for an area with a particular rock type or climate. He further maintained that such characteristic slopes do not necessarily reflect limiting or threshold slopes, which he considered to define changes in the nature of slope-forming processes. Despite Young's (1961) classic distinction between characteristic and limiting slopes, the form and modes of hillslope gradient distributions are still used to argue for the development of threshold hillslopes.

Carson (1969) approached the problem of controls on the angle of straight slope segments through comparison of observed slopes and the range of slopes predicted to be stable for cohesionless soil at dry and saturated conditions. Carson (1969) adopted Skempton's (1964) contention that cohesion tends to be negligible over geologic time and that therefore the only long-term source of slope stability is friction. Hence, the limiting angle of a soil-mantled threshold slope can be derived from the infinite-slope stability model for a cohesionless soil:

$$\tan \theta = [1 - (u/\rho_s g z \cos^2 \theta)] \tan \phi \tag{4}$$

where u is the pore-water pressure, ρ_s is the saturated bulk density of the soil, g is gravitational acceleration, and z is the soil thickness. For the case of slope-parallel subsurface flow through the soil, the pore-water pressure varies linearly with depth:

$$u = \rho_w g h \cos^2 \theta \tag{5}$$

where h is the height of the water table above the base of the soil. Substituting this expression for pore-water pressure into eq (4) yields:

$$\tan \theta = [(\rho_s - (h/z)\rho_w)/\rho_s] \tan \phi \tag{6}$$

where h/z is the proportion of the soil thickness that is saturated.

Carson (1969) proposed that h/z = 0 and h/z = 1 define limiting cases for the development of threshold slopes controlled by stability of the soil mantle. Many subsequent studies of soil-mantled slopes showed that hillslope gradient distributions span the range of about $\phi/2$ to ϕ, as would be predicted to correspond to h/z = 0 to h/z = 1 for the general case where $\rho_s/\rho_w \approx 2$ (Carson and Petley, 1970; Carson, 1971; Rouse, 1975; Dunkerly, 1976; Rouse and Farhan, 1976; Chandler, 1982; Van Asch, 1983; Francis, 1987). Carson (1975) further argued that variability in ϕ gives rise to distributions of threshold slopes, and hence that use of a single threshold slope is unrealistic. Freeze (1987) extended the approach to examine the role of climate and hydraulic conductivity on soil properties and setting maximum stable slope angles. All these studies conclude that landsliding limits slopes to at most the threshold angle(s), but they do not preclude the occurrence of slopes lower than the range of predicted threshold slopes—Strahler's (1950) slopes reduced by wash and creep. In addition, the soil moisture term (h/z) implies that the slope distribution should change with

hydrologic or climatic changes, with, for example, a wetter climate leading to a lower mean slope.

Bedrock threshold hillslopes.—Selby (1980, 1982, 1987) championed the argument that rock mass strength controls the form of weathering-limited bedrock slopes. Selby's studies as well as that of Moon (1984) concluded that adjustment of hillslope gradients to rock strength is widespread based on corelations between rock mass strength and the gradients of bedrock slopes. However, Selby (1987) also recognized that both structurally controlled and soil-mantled (and therefore transport-limited) slopes can occur at gradients less than the limiting slope determined by rock mass strength. Indeed, a general relation between erosive potential and slope would result in more erosion resistant rocks having steeper slopes than more erodible rocks to maintain the same erosion rate across a lithologically variable landscape.

Schmidt and Montgomery (1995) demonstrated that mountain-scale rock strength can limit relief development and hence that bedrock hillslopes may be threshold slopes. They used Culmann's two dimensional, limit equilibrium slope stability model to predict the maximum stable hillslope height (H_c) as a function of hillslope gradient:

$$H_c = (4C \sin \theta \cos \phi / \rho g[1 - \cos (\theta - \phi) \quad (7)$$

where C is the rock cohesion. They fit eq (7) to the maximum envelope defined by slope height and gradient data from stable hillslopes and bedrock landslides in the Santa Cruz Mountains and the Northern Cascades and found that the calibrated C and ϕ values coresponded to measured values for the weakest members of the formations in question. They argued that mountain scale bedrock strength properties, as defined by both the effective large-scale cohesion and friction angle, could define a "limit to topographic development (LTD) beyond which incision of valley bottoms will induce bedrock landsliding that lowers peak elevations" (Schmidt and Montgomery, 1995, p. 618). A landscape incised to its LTD would have threshold hillslopes of a size set by bedrock strength, and that therefore would erode at a rate set by the rate of river incision. Burbank and others (1996) demonstrated this concept by establishing that the gorge of the Indus River had strong gradients in incision rate, but that the mean hillslope gradients were independent of the local river incision rate. Hence, Burbank and others (1996) concluded that the area exhibited threshold hillslopes on which bedrock landsliding allowed efficient adjustment of slope profiles and ridgetop lowering in response to rapid bedrock river incision.

A number of workers have incorporated threshold slope concepts into hillslope evolution models through non-linear transport laws that increase rapidly toward some limiting slope angle (Andrews and Bucknam, 1987; Anderson and Humphrey, 1990; Howard, 1994; Dietrich and Montgomery, 1998). Such models predict the development of relatively linear slopes and skewed slope distributions with a high proportion of slopes at just under the threshold angle (Roering, Kirchner, and Dietrich, 1999). Nonetheless, a normal distribution of hillslope gradients with mean values similar to friction angles characteristic of coarse soils has been taken as *prima facie* evidence for bedrock threshold hillslopes (Burbank and others, 1996; Whipple, Kirby, and Brocklehurst, 1999). Anderson and others (1980), however, cautioned against the use of modal values or peaks of slope distributions as evidence of threshold slopes, and it remains an open question as to what DEM-derived attributes provide a compelling test for the attainment of threshold hillslopes.

STUDY AREAS

The Olympic Mountains and the Oregon Coast Range were selected for analysis of drainage area-slope relations and slope distributions because they represent different structural and geomorphic environments in a comparable climatic setting and for

which 10 m grid size DEMs were available for the whole range. Also, additional independent evidence is available as to whether these ranges are in steady state and may have threshold hillslopes.

The Olympic Mountains (OM) are thought to have been in a tectonic steady state since the Late Miocene and a topographic steady state for much of that time (Brandon, Roden-Tice, and Garver, 1998; Pazzaglia and Brandon, 2001). A regional unconformity and sedimentological evidence for the onset of unroofing constrain accelerated rock uplift in the OM to have commenced between 17 and 12 Ma (Tabor and Cady, 1978; Brandon, Roden-Tice, and Garver, 1998). Brandon, Roden-Tice, and Garver (1998) report extensive fission track dating of samples derived from a wide range of elevations in the OM and conclude that rock uplift since then has remained steady, although rock uplift rates vary from 0.3 mm/yr on the fringes of the range to >0.7 mm/yr in the center of the range (Brandon, Roden-Tice, and Garver, 1998; Pazzaglia and Brandon, 2001). Given the long period of tectonic steady state, they conclude that the OM are in topographic steady state. Pleistocene alpine glaciers carved large valleys in the core of the range (Montgomery and Greenberg, 2000), leaving steep bedrock valley walls. Numerous spreading ridgetops and large bedrock landslides occur in both the core of the OM and the eastern end of the range (Tabor, 1971; Gerstel 1999).

The Oregon Coast Range (OCR) is also thought to be in topographic steady state, although lower rock uplift rates have resulted in more subdued topography than in the OM. The Eocene Tyee Formation, which composes much of the OCR was deposited in a deltaic environment on a narrow continental shelf (Dott and Bird, 1979). Like the OM, uplift of the OCR also began in the Miocene (McNeill and others, 2000). There is little sediment storage in the valley system of the OCR, and based on comparison of Holocene hillslope erosion rates to contemporary river sediment yields Reneau and Dietrich (1991) concluded that the OCR was in erosional steady-state. Rock uplift rates determined from both geodetic data and marine terrace elevations vary along the coast, falling from the south to central OCR and then rising again to the northern OCR (Kelsey and others, 1994). Bedrock river incision rates determined from dating of strath terraces also imply that the central OCR has lower uplift rates than the northern or southern OCR (Personius, 1995). The OCR was not glaciated in the Pleistocene, although the inferred climate was cooler and wetter than in the Holocene (Worona and Whitlock, 1995). Shallow landsliding of the soil mantle is an important sediment transport process in the OCR (Dietrich and Dunne, 1978), but deep-seated bedrock landslides are relatively uncommon. Shallow landslides in the OCR typically originate in colluvium-filled bedrock hollows at the head of the channel network (Dietrich and others, 1986; Montgomery and Dietrich, 1988). Although industrial forestry throughout much of the OCR has accelerated rates of shallow landsliding (Brown and Krygier, 1971; Beschta, 1978; Montgomery and others, 2000), the impact would not influence slope form on the scale considered in this analysis.

METHODS

The available 10 m grid DEMs, derived from contour coverages from United States Geological Survey 1:24,000 scale topographic maps, were combined to form continuous coverages for each of the study areas. The composite DEMs were processed using standard pit filling algorithms to allow unique determination of downslope flowpaths. Drainage areas were determined with a new approach in which drainage areas less than 10^4 m^2 were calculated using custom programs to determine specific catchment areas (drainage area per unit contour width) following Costa-Cabral and Burges (1994). To account for routing of flow through channels defined at sub-pixel resolution, drainage areas greater than 10^4 m^2 were calculated using the D8-equivalent algorithm employed by ARC/INFO. Local slopes were determined from the steepest descent between neighboring grid cells. In this manner, paired drainage area and

slope values were calculated for each grid cell in both mountain ranges. In addition, analyses of the hillslope gradient distributions were conducted by generating the distributions of slopes determined from individual 10-m grid cells for a larger 10 by 10 km grid and the mean slope values for a 10 km diam window centered on each grid cell in the range.

Slope stability analysis.—Comparison of mapped landslides to predictions of a model that combines topographically-driven hydrologic models with slope stability models reveals that such models can provide a reasonable measure of the relative potential for shallow landsliding (Montgomery, Greenberg, and Sullivan, 1998; Montgomery and others, 2000). Unfortunately, no comparable model for bedrock landslide potential is available at present. The approach used in this analysis couples a steady-state hydrologic model to a limit-equilibrium slope stability model to calculate the critical steady-state rainfall necessary to trigger slope instability at any point in a landscape. The hydrologic model assumes that flow infiltrates to a lower conductivity layer and follows topographically-determined flow paths to map the spatial pattern of equilibrium soil saturation based on analysis of upslope contributing areas, soil transmissivity, and local slope (O'Loughlin, 1986). Specifically, local soil wetness is calculated as the ratio of the local flux at a given steady-state rainfall to that upon complete saturation of the soil profile. Combining this hydrologic model with the infinite-slope stability model for cohesionless soils provides a simple model for the critical steady-state rainfall required to cause slope instability (Q_c):

$$Q_c = [T \sin \theta/(a/b)] + (\rho_s/\rho_w)[1 - (\tan \theta/\tan \phi)] \quad (8)$$

where a is the upslope contributing area, b is the contour length across which flow is accounted for, and T is the soil transmissivity, which is given by the product of the soil thickness and hydraulic conductivity (Montgomery and Dietrich, 1994). Recalling eq (6), slopes that are stable even when $h/z = 1$ are interpreted to be unconditionally stable and to require excess pore pressures to generate slope instability, as there is no mechanism in this model for generating pore pressures greater than hydrostatic (that is, $h/z > 1$). Similarly, slopes predicted to be unstable even when dry (that is, $h/z = 0$) are considered to be unconditionally unstable areas where soil accumulation would be difficult. Critical rainfall values can be calculated for slopes for which the critical value of h/z varies between 0 and 1, which correspond respectively to slopes between $\tan \theta = \tan \phi$ for $h/z = 0$ and $\tan \theta = \tan \phi\,[1 - (\rho_s/\rho_w)]$ for $h/z = 1$. This range of slopes corresponds to that proposed by Carson (1969) to define limiting bounds to the range of angles for threshold soil-mantled hillslopes. The formulation cast in terms of Q_c allows assessing the relative role of topographic forcing on soil moisture and therefore the relative probability of landsliding across an entire landscape.

RESULTS

Our analysis reveals similarities in both the drainage area-slope relationship and the general patterns of slope distributions for the two ranges. However, distributions of Q_c values and spatial gradients in mean slope values differ between the ranges in ways directly related to the interpretation of whether each range has threshold hillslopes.

Drainage area-slope relations.—The huge number of grid cells for the composite DEMs of these ranges (126 million for the Olympics, 267 million for the Oregon Coast Range) precludes simple visual examination of drainage area-slope relations from plots of all the individual grid cells in either range. However, a contour plot of the density of data allows assessment of patterns in each data set. Most grid cells occur on slopes greater than 0.1 and at relatively small drainage areas (fig. 4). No simple relationships like those predicted by eq (3) are apparent for either range, as there is tremendous scatter across almost the full range of drainage areas and slopes. However,

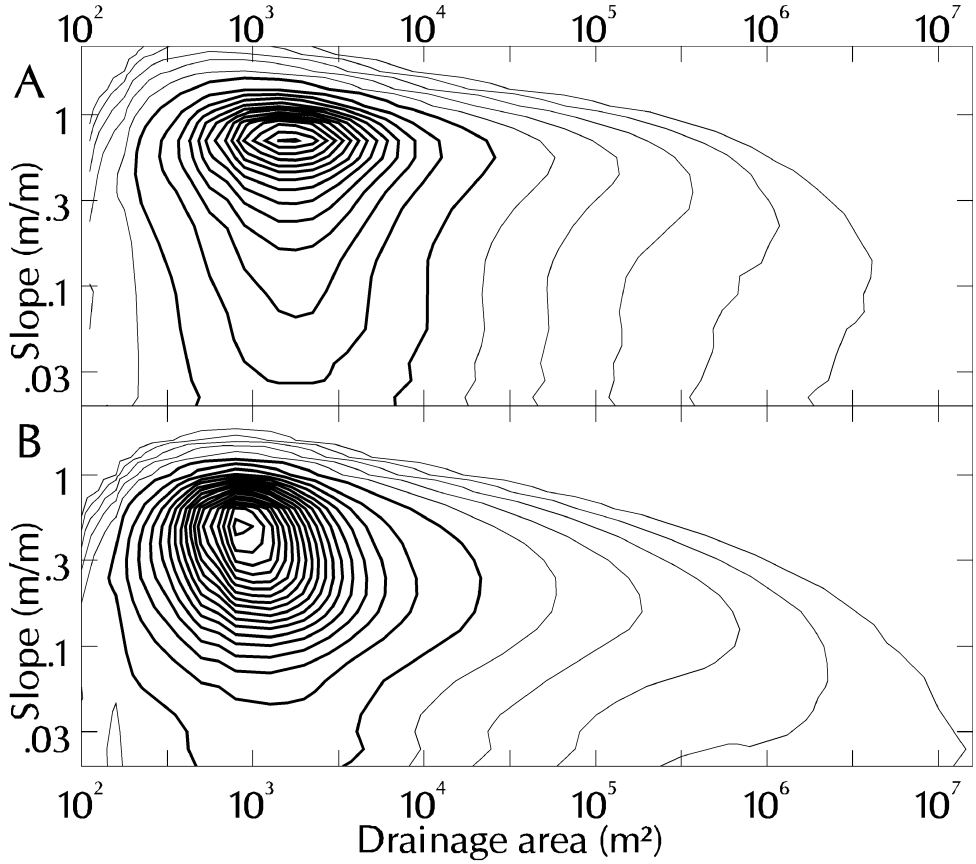

Fig. 4. Contour plots of the density of drainage area versus slope data for (A) Olympic Mountains and (B) Oregon Coast Range. Data density contours expressed in the number of 10 m grid cells that fall within bins of 0.1 log units along each axis. Major contours for the Olympic Mountains data represent 100,000 grid cells; minor contours are for values of 3225, 6250, 12500, 25,000, and 50,000 grid cells. Major contours for the Oregon Coast Range data represent 160,000 grid cells; minor contours are for values of 5000, 10000, 20000, 40000, and 80000 grid cells.

the central tendency of the data, as illustrated by the shape and apices of the density contours, generally conforms to the predictions of eq (4). Both mountain ranges show poorly-defined positive and inverse trends to data on either side of a "bulls eye" concentration of data at approximately the hillslope-valley transition. The overall distibution of data has an attractor at the scale of the transition from hillslopes to valleys, with additional data at low slope and drainage areas, likely formed by valley walls, terraces, and floodplains, and a tail of data at high drainage areas along the channel network. In addition, note that the OCR data is more symetrically distributed around the attractor than the OM data, which appear compressed in the vertical dimension—as if the hillslopes were approaching a limit to how steep they could stand.

The variance of almost an order of magnitude in slope for a given drainage area likely reflects that the composite data for an entire mountain range incorporates areas with different climate and rock uplift rates. Some of the variance also reflects that different erosional processes occur in locations that plot in different portions of a drainage area-slope graph (Dietrich and others, 1992; Montgomery and Foufoula-Georgiou, 1993). Plotting data from a variety of such areas on the same graph may

serve to obfuscate any systematic drainage area-slope relationships for individual process domains (that is, areas dominated by hillslope, debris flow, or fluvial processes). In addition, areas underlain by different lithologies may introduce additional scatter to the composite data set through variations in K, which may vary over several orders of magnitude (Stock and Montgomery, 1999). Together these sources of variability would be expected to impart substantial variability in slope for a given drainage area even within steady-state topography.

Nonetheless, ploting the mean slope values for data from each 0.1 log unit bin of drainage area results in the expected transition from a positive trend for low drainage areas (hillslopes) to an inverse relation for larger drainage areas (channels) (fig. 5). The slope of these mean values is not constant but exhibits a series of ranges characterized by approximately log-linear segments. Mean slope values from each range rise from low values at the drainage area of a single grid cell (100 m^2) to high values at drainage areas of 800 to 900 m^2. Although these data do not follow a linear trend, the exponents for these data are close to unity. At larger drainage areas, four zones of approximately log-linear scaling are apparent. The first three zones exhibit similar exponent values in both the OM and OCR, but the fourth zone, at the greatest drainage areas, exhibits very different exponent values. Aside from this striking difference, the form of the data from these two ranges is very similar. However, the data from the OM are consistently steeper for the same drainage area than data from the OCR, and the shoulder to the data that defines the hillslope-valley transition is broader in the OM than in the OCR.

Slope distributions.—Both study areas exhibit an essentially bimodal pattern of normal and exponential distributions at the scale of the 10 km grid (fig. 6 and 7). Normal and exponential distributions provide apt first-order descriptions of most of the slope distributions, although a few of the individual distributions are multi-modal, left- or right-skewed. In the Olympic Mountains, the core of the range has normal slope distributions, and exponential distributions characterize depositional environments, such as large alluvial valley bottoms and areas on the fringes of the range buried by glacial outwash and/or overrun by continental ice sheets. Mean slopes are greater in the core of the range, where they are uniformly 28° to 32°. In the Oregon Coast Range, normal and left-skewed distributions are prevalent along the central spine of the range, and exponential distributions are prevalent on the eastern end of the range along the Willamette Valley, in the lower elevation portions of the northern end of the range, and along the Pacific coast. Mean slopes in the OCR exhibit substantial latitudinal variation, with 20° to 24° mean slopes in the southern portion of the range, mean slopes of $<20°$ in the central portion of the range, and steeper mean slopes of 23° to 31° in the northern part of the range.

Slope stability analysis.—Slope stability modelling using eq (8) reveals differences in the proportions of landslide susceptible areas in the study ranges (fig. 8). For the Olympic Mountains. most of the length of the valley walls in the core of the range are in Q_c categories predicted to represent high probability of slope failure ($Q_c \leq 100$ mm day^{-1}). In contrast, the pattern of relative slope instability in the Oregon Coast Range shows that areas of potential instability are localized in steep headwater valleys, particularly at the heads of the channel network (Montgomery and Dietrich, 1994). Differences among the study areas are further illustrated by the different distributions of Q_c values for the drainage basins from each range. One-half the potentially unstable ground (that is, the area not considered unconditionally stable) is within the lowest critical rainfall categories for the OM, supporting the interpretation that the OM have a high degree of threshold slope development. In contrast, the Oregon Coast Range shows the opposite asymmetry, with few slopes steep enough to be considered chronically unstable ($Q_c = 0$), and only one-fifth of the range in the three lowest Q_c

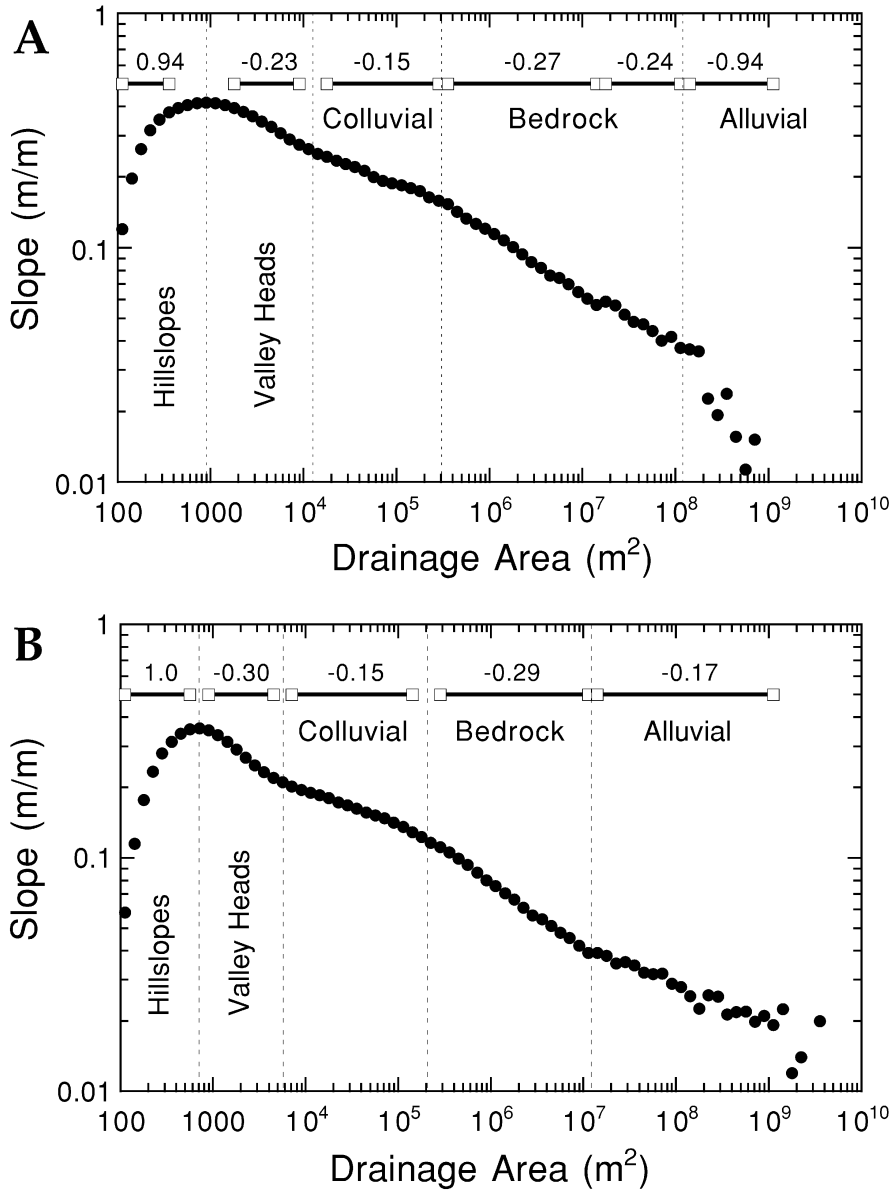

Fig. 5. Plot of log-bin averaged drainage area versus slope relationship derived from data in figure 4 for (A) Olympic Mountains and (B) Oregon Coast Range. The plot shows the mean slope of the individual 10 m grid cells for each 0.1 log interval in drainage area. Numbers show the exponent for a power function regression of values in the segments of the plots indicated by bars connecting open squares. Dashed vertical lines divide the plot into areas considered to reflect different geomorphic zones of the landscape, or process domains, as characterized by labels on the figure.

(highest hazard) categories. While sediment transport in the OCR may be dominated by shallow landsliding, most OCR hillslopes are less likely to be threshold hillslopes than are OM hillslopes.

Transect analysis.—Profiles of the mean elevation and mean slope across each range show different general relationships between these ranges (fig. 9). As noted by

Fig. 6

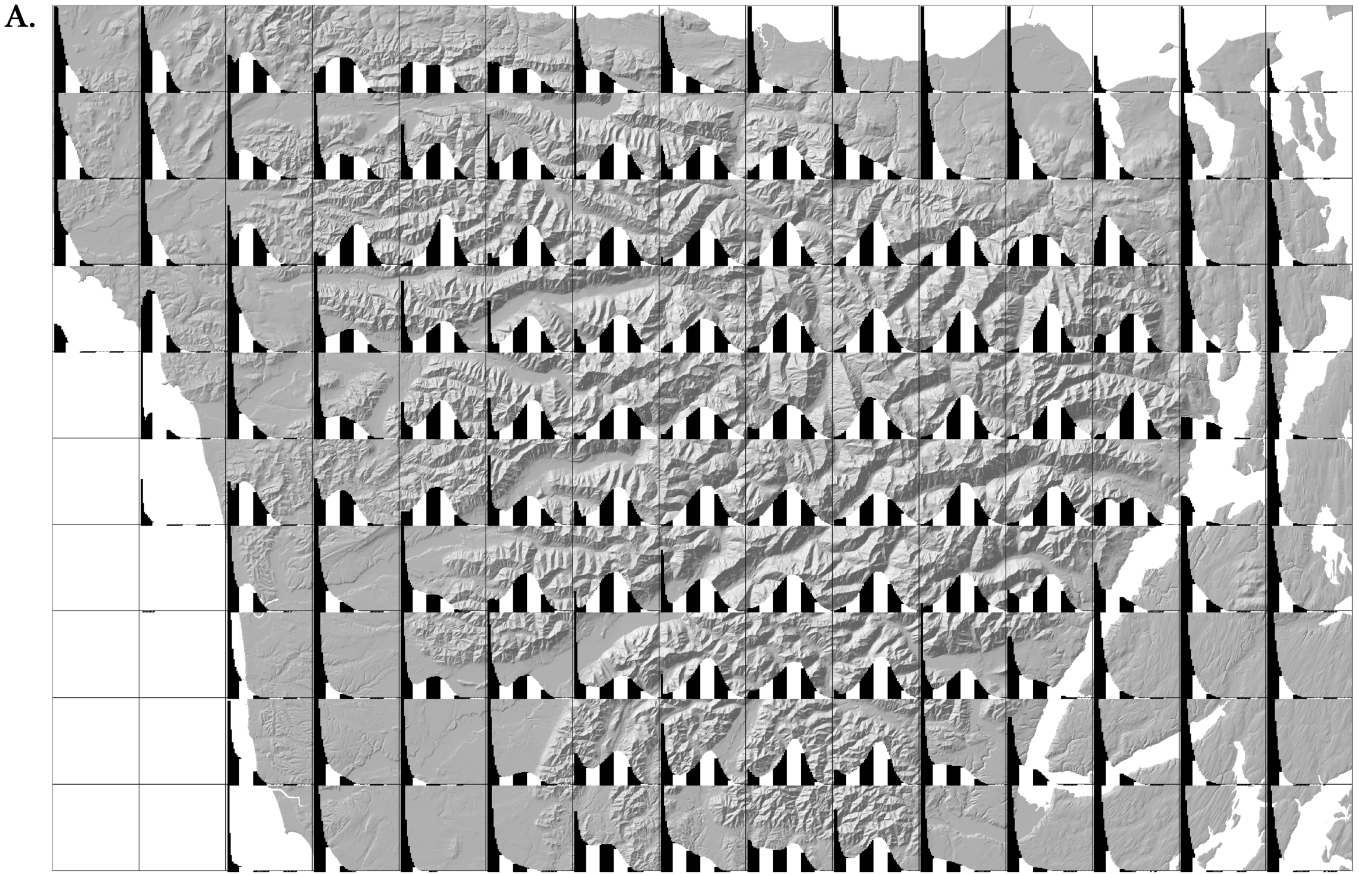

(A) Topography of the Olympic Mountains and slope frequency histograms showing the distribution of individual 10 m grid cell slopes for a 10 by 10 km grid—shading of the slope distributions changes from black to white at 10° slope intervals.

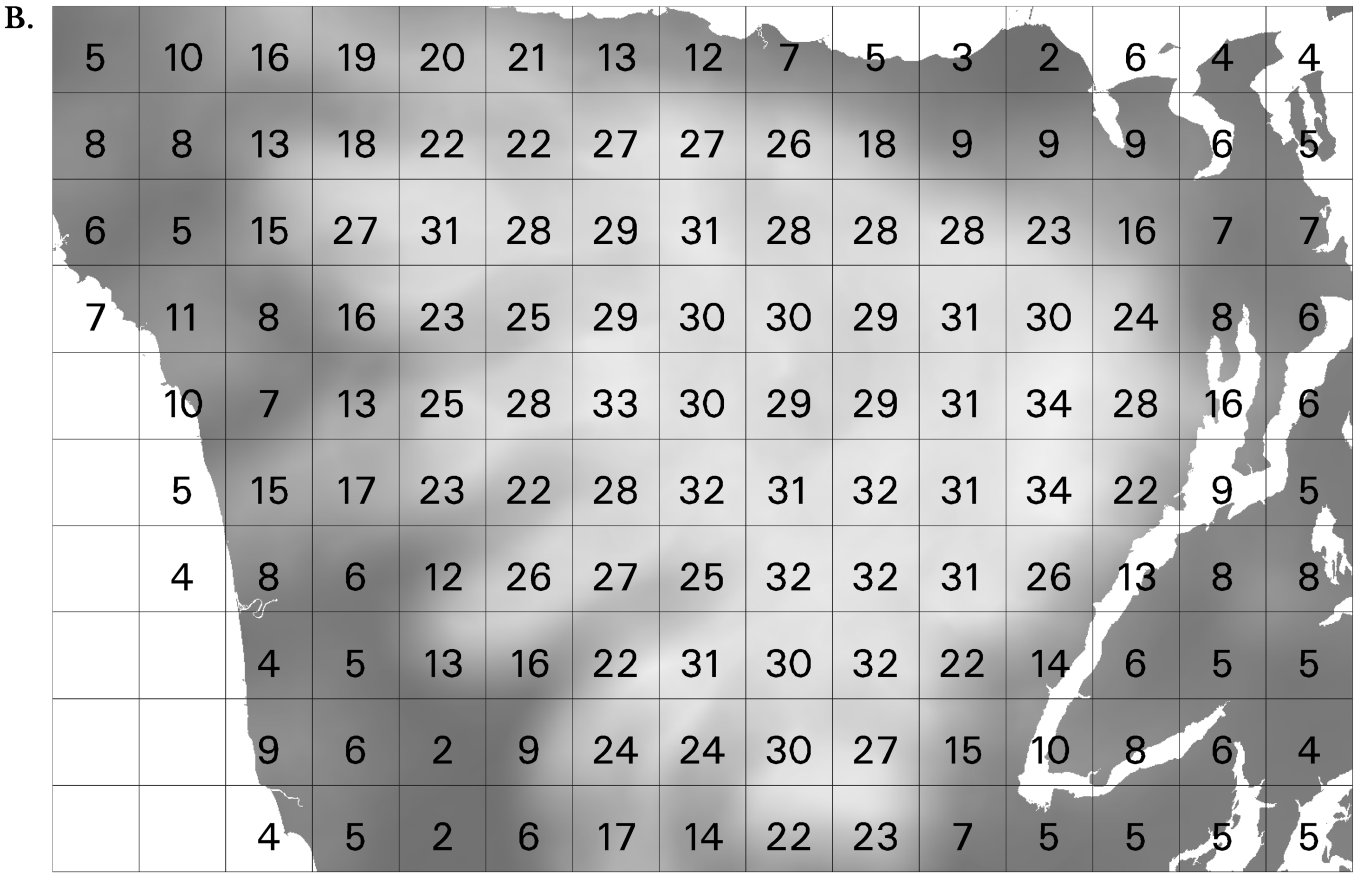

(B) mean slope values within each 100 km^2 grid cell —shading shows distribtion of mean slope values for a 10 km diam. window centered on each 10 m grid cell.

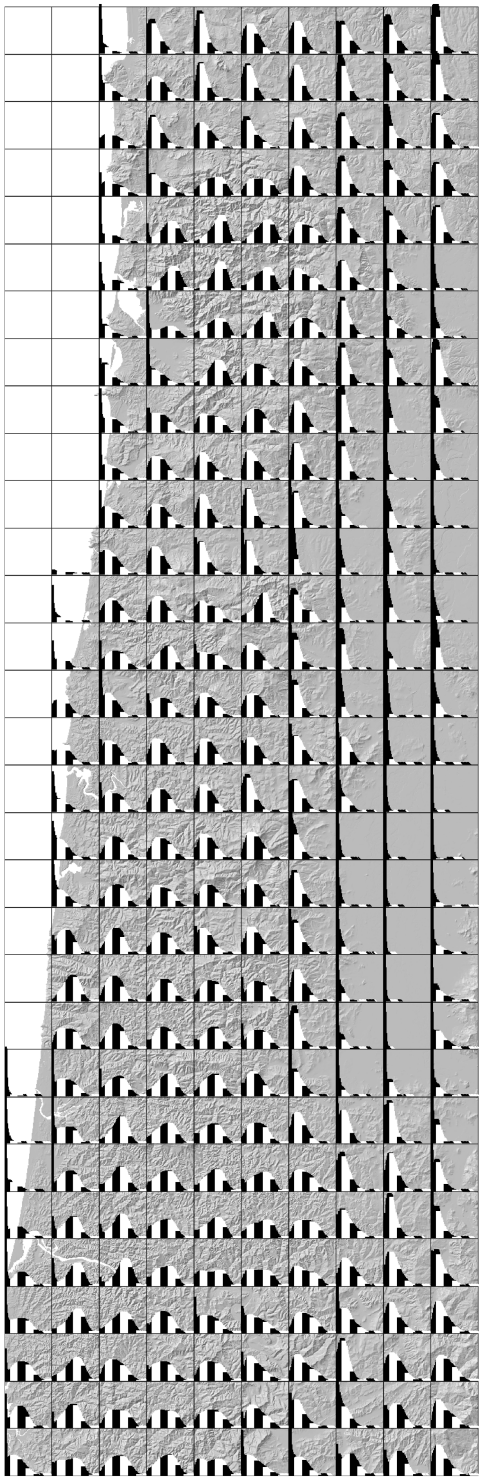

		6	12	12	16	13	12	12	10
		13	17	15	11	12	10	11	9
		19	15	16	13	15	12	11	13
		19	16	25	24	16	12	13	14
		13	27	31	30	23	14	12	11
		18	31	32	28	20	14	7	2
		10	16	28	29	21	13	9	3
		12	10	29	22	17	11	8	10
		15	17	22	20	15	9	4	7
		13	17	17	17	14	10	2	3
		16	18	15	12	10	4	4	1
	16	16	15	12	10	5	2	6	1
	7	19	18	19	24	15	4	5	2
	12	21	25	19	16	10	5	4	6
	14	13	19	19	18	10	4	2	4
	15	16	18	18	15	12	10	3	2
	11	18	19	17	11	12	6	1	0
	12	22	21	18	18	8	1	1	1
	11	23	21	20	17	12	1	1	2
	18	21	22	15	18	11	2	1	4
	25	20	23	23	21	15	3	1	6
	21	21	22	24	22	10	3	1	8
3	17	22	25	24	18	9	2	3	4
3	17	26	25	23	21	14	10	9	5
7	20	25	24	26	24	19	12	13	8
13	23	26	23	25	25	23	15	12	8
15	26	31	23	23	23	20	17	14	13
16	29	28	22	18	18	22	13	14	16
21	28	22	21	23	17	20	11	16	20
18	24	25	25	24	20	13	9	16	18
14	23	25	25	23	15	12	16	17	15

Fig. 7 (Left) Topography of the Oregon Coast Range and slope frequency histograms showing the distribution of individual 10 m grid cell slopes for a 10 by 10 km grid—shading of the slope distributions changes from black to white at 10° slope intervals; (Right) mean slope values within each 100 km^2 grid cell —shading shows distribtion of mean slope values for a 10 km diam. window centered on each 10 m grid cell.

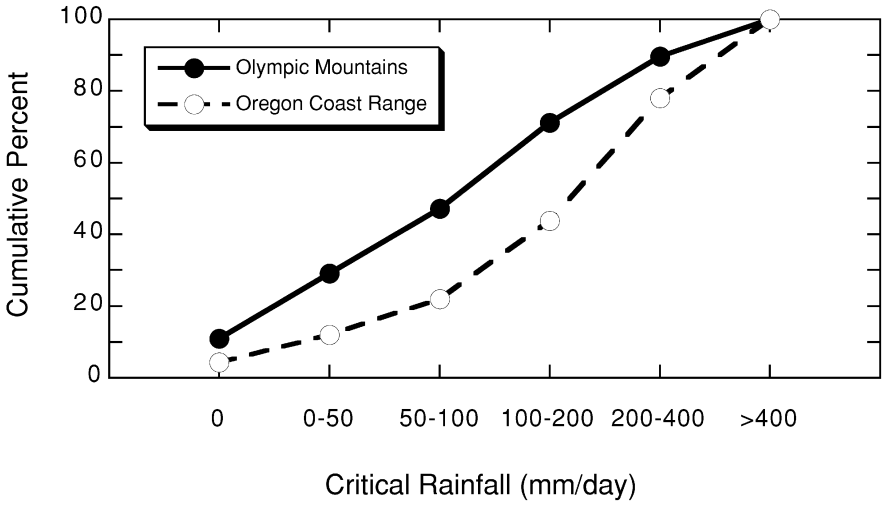

Fig. 8. Percentage of potentially unstable ground in each critical rainfall category for the study ranges, using $\phi = 45°$, $\rho_s/\rho_w = 2$, and $T = 65\ m^2\ day^{-1}$.

Montgomery and Greenberg (2000), the mean slope across the core of the Olympic Mountains is relatively constant even though rock uplift rates vary substantially (Brandon, Roden-Tice, and Garver, 1998)—implying either the development or close approximation of threshold bedrock slopes. In the Oregon Coast Range, mean slopes vary substantially, falling from the southern end of the range toward the central portion and rising again in the northern portion of the range. This pattern parallels variation in both rock uplift rates noted by Kelsey and others (1994) and bedrock stream incision documented by Personius (1995), coupled with a greater local erosion resistance of basalt in portions of the northern part of the range. As the mean elevation does not vary substantially along the OCR, it appears that these changes in slope are a primary landscape adjustment to both gradients in rock uplift and to differential erodibility.

DISCUSSION

The similarities and differences in the drainage area-slope relationships and slope distributions for the OM and OCR are consistent with both ranges being steady-state topography. These two ranges have similar general patterns and large variability in the drainage area-slope relations and a general tendency for local slope distributions to exhibit either normal or exponential distributions. However, within range patterns of variability are consistent with different relations between threshold hillslopes and steady-state topography.

Drainage area-slope plots.—The most striking characteristic of the drainage area-slope plots of each range is the attractor at drainage areas of one to several thousand square meters. This range in drainage areas is similar to the range of drainage areas necessary to support a channel head in the OCR (Montgomery and Dietrich, 1988, 1992). Hence, the hillslope-channel transition not only sets the length scale of landscape dissection but also acts as an attractor around which the drainage area-slope characteristics of the landscape self organize. While there is intrinsic variability around this attractor, most of the landscape is organized around the length scale of the hillslope-channel transition, with a "tail" that extends down large river valleys.

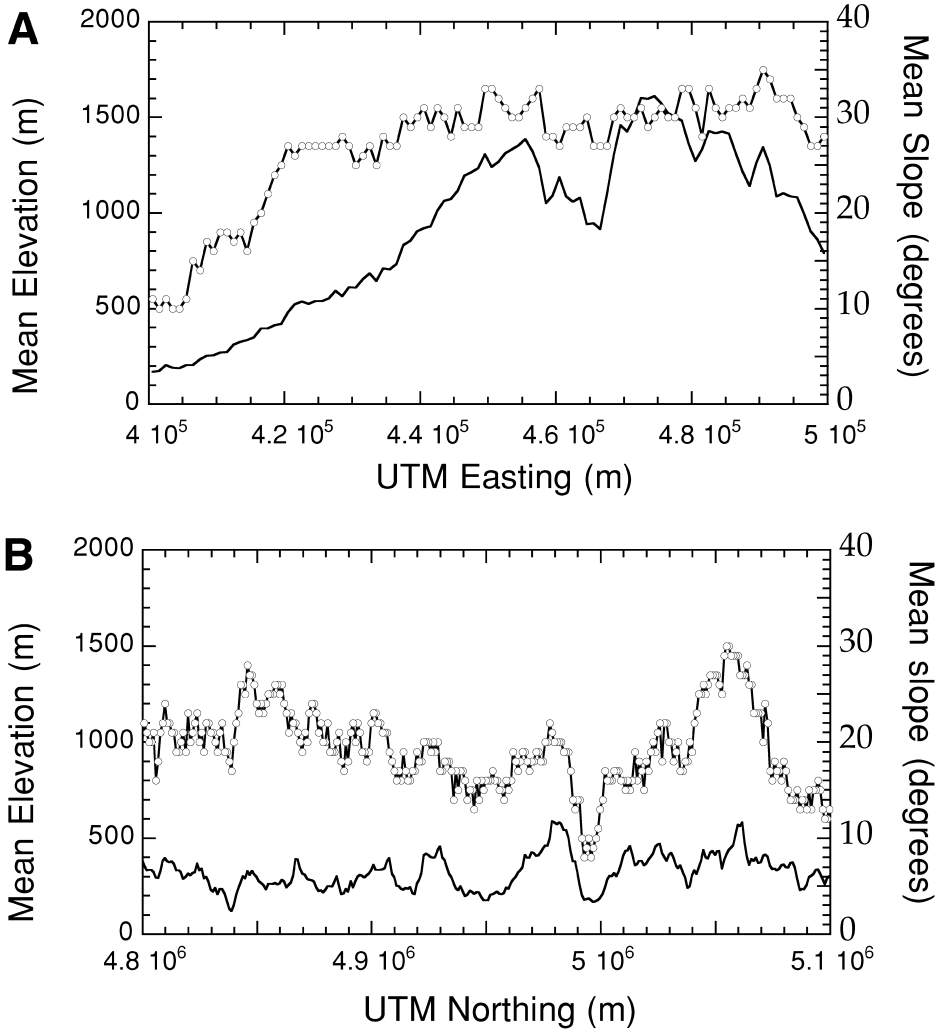

Fig. 9. Transects of the study ranges showing the mean elevation and mean slope (open circles) calculated for 1 km increments (A) across the Olympic Mountains and (B) along the Oregon Coast Range.

Several things likely contribute to the substantial scatter to range-wide drainage area and slope data. Various processes shape different parts of a drainage basin—hillslopes, debris-flow-prone hollows and headwater colluvial channels, bedrock channels, and alluvial channels are all likely characterized by different process laws and therefore different values of m and n. In addition, K values for bedrock river incision may differ by orders of magnitude between different rock types (Stock and Montgomery, 1999). Moreover, the contemporary topography may reflect forms inherented from glacial land sculpting, and rock uplift rates may not be uniform across a range that is in steady state (Brandon, Roden-Tice, and Garver, 1998; Pazzaglia and Brandon, 2001). Hence, it is difficult to evaluate how much of the scatter in range-wide drainage area-slope plots simply reflects spatial variability in rock uplift rates, erosional processes, or erosion resistance. Considering that such scatter may reflect spatial variability in m/n U/K, transient variations that average out over geologic time, DEM artifacts,

and/or that the range might not actually be in steady state, how much variability in both space and time is permissible for a mountain range to be considered in topographic steady state?

The five zones of different drainage area-slope scaling relations apparent on figure 5 correspond to portions of the landscape characterized by different geomorphological processes. The positive relation for data at drainage areas of 10^2 to 10^3 m^2 corresponds to hillslopes dominated by primarily slope-dependent transport processes. The second region, from 10^3 to about 10^4 m^2, corresponds to the scale of valley heads across which the hillslope-channel transition occurs. These drainage areas are similar to the range of drainage areas necessary to support a channel head identified in intensive field surveys in the OCR (Montgomery and Dietrich, 1988, 1992). At a given time, specific locations in these valley heads may be unchanneled valleys and small channels. The next three regions of the plots, respectively, correspond to colluvial, bedrock, and alluvial channel segments. Field mapping in these and other Pacific Northwest mountain ranges has shown that colluvial channel reaches occur at drainage areas of 10^4 to 10^6 m^2 and that bedrock valley segments (which can host a range of channel reach types) typically characterize locations with drainage areas of 10^5 to 10^8 m^2 (Montgomery and Buffington, 1997).

Assuming that the range is in steady state and that rock uplift rates are uniform across each range, power law regressions of the data to either side of the hillslope/valley transition would yield estimated m/n values for different portions of these study areas. As rock uplift rates are not uniform within either the OM or the OCR and the data presented here are mean values for the entire landcape, the exponent values for these range-wide plots may differ from the values that would be derived from comparable analyses of individual channel profiles. Snyder and others (2000) also noted different drainage area-slope relations for channel profiles through colluvial, bedrock, and alluvial channel segments derived from 30 m grid DEMs, but the exponent values of about 0.43 that they found for bedrock channel segments are greater than those reported here. Although it is difficult to imagine grid cells with drainage areas greater than 1 km^2 (10^6 m^2) not representing a channel, the relation of the whole-range mean exponent values to specific process law parameterizations is not straightforward. Nonetheless, the consistency in the general form of the drainge area-slope relations between these two mountain ranges argues that five basic process zones, each with its own process law paramaterization, characterize mountain drainage basins.

Slope distributions.—The consistent pattern of locally normal or exponential slope distributions for the 10 by 10 km grids defined for the OM and OCR show that generally normal slope distributions characterize the upland bedrock portions of these mountain ranges, whereas exponential slope distributions characterize the margins of the ranges and areas dominated by depositional landforms. This fundamental difference in the form of erosional and depositional topography in these ranges suggests recasting Strahler's Law as:

> within an area of active bedrock uplift slopes evolve toward a normal distribution the mean of which reflects local processes influencing erosion rates such as to maintain either threshold slopes or slopes in equilibrium with rock uplift rates, whereas slopes tend toward exponential slope distributions in depositional terrain.

The normal distributions of slope gradients for many locations throughout both the OM and OCR demonstrate that, in contrast to the assumption adopted in several recent studies, the development of a normal slope distribution does not itself constitute sufficient evidence for development of bedrock threshold hillslopes. In addition, slope distributions and mean slope values do not vary substantially across the core of the Olympics, despite a two-fold increase in long-term rock uplift rates and basalt in the high elevation eastern portion of the range. As argued by Burbank and others (1996)

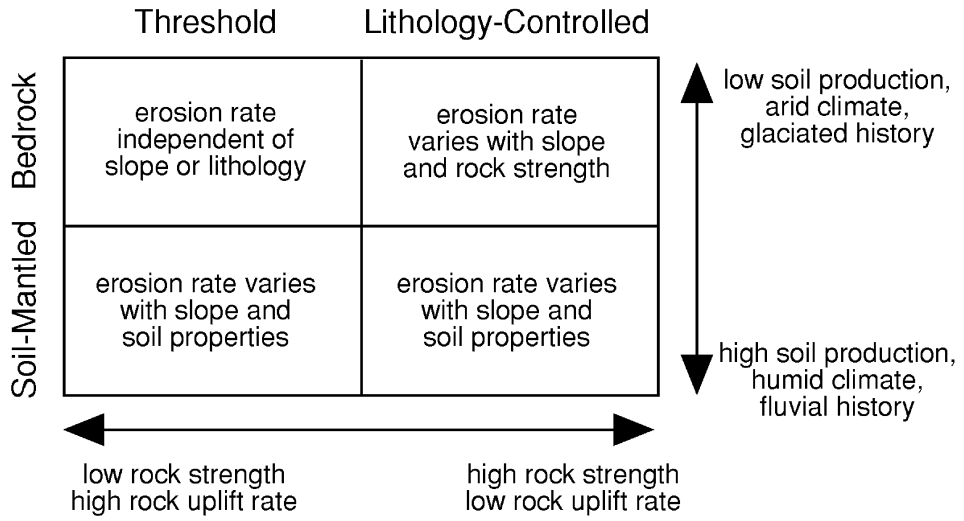

Fig. 10. A classification of hillslope types based on threshold versus lithology-controlled (subthreshold) characteristics and bedrock versus soil-mantled morphology, along with brief descriptions of the expected relationships between slope distributions and rock uplift rates and the types of conditions favoring the development of each of the four types of hillslope so defined.

for the Indus gorge, the independence of the mean slope from the rock uplift rate implies development of bedrock threshold hillslopes. In contrast, the pattern of mean slopes in the Oregon Coast Range tracks variations in both geodetically measured uplift and marine terrace elevations (Kelsey and others, 1994) and bedrock river incision rates (Personius, 1995). This correspondence argues that rates of rock uplift influence hillslope gradients in the Oregon Coast Range, and therefore that although the range may be at steady state, it does not have bedrock threshold hillslopes. Hence, the OCR does not exhibit threshold bedrock slopes. Instead, slope distributions in the OCR likely reflect an equilibrium adjustment to variations in the rock uplift rate and erodibility as mediated by lithology and soil properties.

Types of hillslopes.—The classic conception of threshold slopes is complicated by differences between soil-mantled and bedrock hillslopes. In addition, lithology-controlled (or subthreshold) slopes also can be either bedrock or soil-mantled hillslopes. Hence, we may outline a simple typology for differentiating the resulting four types of hillslopes (fig. 10). In the case of classic soil-mantled threshold slopes, the properties of the soil together with the relative wetness of the soil (h/z), rather than the properties of the underlying bedrock, set the slope angles expressed in the topography (Carson, 1975). The implication is that for soil mantled slopes the climate and failure frequency can affect mean slope angles, which therefore vary across a landscape and through time. In contrast, bedrock threshold hillslopes adjust to variability in rock uplift rates through failure frequency instead of slope morphology. With bedrock threshold hillslopes we expect no correlation between slope and rock uplift rates, whereas in an area with subthreshold slopes we would expect a correlation between mean slope, rock uplift rate, and the material strength properties for both bedrock and soil-mantled hillslopes.

The development of threshold hillslopes in a mountain range depends on both the relative rock uplift rate and the time since that uplift rate commenced. If the rock uplift rate exceeds the erosion rate then slopes will steepen, which will in turn increase erosion rates and eventually lead to an equilibrium hillslope form as long as the rock

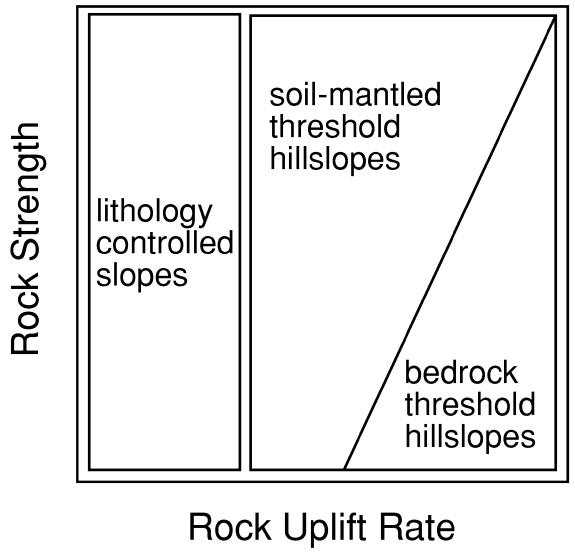

Fig. 11. Schematic relation showing combinations of rock strength and rock uplift rate associated with development of lithology-controlled, soil-mantled threshold, and bedrock threshold hillslopes.

uplift is sustained. Lithology-controlled hillslopes may develop where the rock uplift rate is low enough to be matched by the erosion rate on slopes less than the stability threshold for the slope-forming material. However, if the rock uplift rate is great enough to so steepen slopes as to engage their ultimate mechanical strength, then upon further river incision bedrock landsliding will limit relief development (Schmidt and Montgomery, 1995; Burbank and others, 1996). Once slopes equal the threshold angles, then the rock uplift rate can increase without further changes in mean slope. Hence, we would expect to see a relation between rates of rock uplift and hillslope type: with increasing rock uplift rate, lithology-controlled slopes would give way to soil-mantled threshold slopes, and at high rock uplift rates bedrock threshold slopes.

The interplay between rock uplift, hillslope gradients, and the evolution of threshold slopes should vary over the life of an orogen. Slow rock uplift rates make the role of rock resistance more apparent, and hence we should expect to see differences in mean slope for different rock types until threshold slopes develop. Once sustained high uplift rates drive hillslope gradients to the threshold state, then different rock types or spatial gradients in uplift rates may influence frequency of sliding but not slope morphology. Although the relative roles of rock strength and rock uplift rates in controlling the development of threshold slopes will vary for different orogens (fig. 11), mountain ranges with high rock uplift rates and/or relatively weak rocks (for example, Taiwan or the Himalaya) should exhibit strong bedrock threshold hillslopes, whereas mountain ranges with relatively strong rocks and slow rock uplift rates (for example, Sierra Nevada) should exhibit lithology-controlled hillslopes.

ACKNOWLEDGMENTS

I thank Harvey Greenberg for GIS support and Frank Pazzaglia and Peter Kneupfer for the invitation and encouragement to develop these ideas. I also thank Joshua Roering for his very insightful and helpful critique of the manuscript.

References

Anderson, M. G., Richards, K. S., and Kneale, P. E., 1980, The role of stability analysis in the interpretation of the evolution of threshold slopes: Institute of British Geographers, Transactions, New Series, v. 5, p. 100-112.

Anderson, R. S., and Humphrey, N. F., 1989, Interaction of weathering and transport processes in the evolution of arid landscapes, *in* Cross, T. A., editor, Quantitative Dynamic Stratigraphy, Englewood Cliffs, Prentice Hall, pp. 349-361.

Andrews, D. J., and Bucknam, R. C., 1987, Fitting degradation of shoreline scarps by a nonlinear diffusion model: Journal of Geophysical Research, v. 92, p. 12,857-12,867.

Avouac, J.-P., and Burov, E.B., 1996, Erosion as a driving mechanism of intracontinental mountain growth: Journal of Geophysical Research, 101, v. 8, p. 17,747-17,769.

Beaumont, C., Fulsack, P., and Hamilton, J., 1991, Erosional control of active compressional orogens, *in* McClay, K. R., editor, Thrust Tectonics, New York, Chapman and Hall, p. 1-18.

Beschta, R. L., 1978, Long-term patterns of sediment production following road construction and logging in the Oregon Coast Range: Water Resources Research, v. 14, p. 1011-1016.

Brandon, M. T., Roden-Tice, M. K., and Garver, J. I., 1998, Late Cenozoic exhumation of the Cascadia accretionary wedge in the Olympic Mountains, northwest Washington State: Geological Society of America Bulletin, v. 110, p. 985-1009.

Brown, G. W., and J. T. Krygier, 1971, Clear-cut logging and sediment production in the Oregon Coast Range: Water Resources Research, v. 7, p. 1189-1198.

Burbank, D. W., Leland, J., Fielding, E., Anderson, R. S., Brozovic, N., Reid, M. R., and Duncan, C., 1996, Bedrock incision, rock uplift and threshold hillslopes in the northwestern Himalayas: Nature, v. 379, p. 505-510.

Carson, M. A., 1969, Models of hillslope development under mass failure: Geographical Analysis, v. 1, p. 77-100.

——— 1971, An application of the concept of threshold slopes to the Laramie Mountains, Wyoming, Institute of British Geographers Special Publication 3, p. 31-47.

——— 1975, Threshold and characteristic angles of straight slopes, *in* Mass Wasting, Proceedings of the 4th Guelph Symposium on Geomorphology, Norwich, United Kingdom, GeoAbstracts, p. 19-34.

——— 1976, Mass-wasting, slope devlopment and climate, *in* Derbyshire, E., editor, Geomorphology and Climate, London, John Wiley & Sons, p. 101-136.

Carson, M. A., and Petley, D. J., 1970, The existence of threshold hillslopes in the denudation of the landscape: Institute of British Geographers, Transactions, v. 49, p. 71-95.

Chandler, R. J., 1982, Lias clay slope sections and their implications for the prediction of limiting or threshold slope angles: Earth Surface Processes and Landforms, v. 7, p. 427-438.

Costa-Cabral, M. C., and Burges, S. J., 1994, Digital elevation model networks (DEMON): A model for flow over hillslopes for computation of contributing and dispersal areas: Water Resources Research, v. 30, p. 1681-1692.

Davis, W. M., 1892, The convex profile of bad-land divides: Science, v. 200, p. 245.

——— 1898, The grading of mountain slopes: Science, v. 7, p. 81.

——— 1899, The geographical cycle: Geographical Journal, v. 14, p. 481-504.

Dietrich, W. E., and Dunne, T., 1978, Sediment budget for a small catchment in mountainous terrain: Zeitschrift für Geomorphologie, Supplementband 29, p. 191-206.

Dietrich, W. E., and Montgomery, D. R., 1998, Hillslopes, channels, and landscape scale, *in* Sposito, G., editor, Scale Dependence and Scale Invariance in Hydrology, Cambridge, Cambridge University Press, p. 30-60.

Dietrich, W. E., Wilson, C. J., Montgomery, D. R., McKean, J., and Bauer, R., 1992, Channelization Thresholds and Land Surface Morphology: Geology, v. 20, p. 675-679.

Dietrich, W. E., Wilson, C. J., and Reneau, S. L., 1986, Hollows, colluvium, and landslides in soil-mantled landscapes, *in* Hillslope Processes, Abrahams, A. D., editor, London, Allen and Unwin, p. 361-388.

Dott, R. H., Jr., and Bird, K. J., 1979, Sand transport through channels across an Eocene shelf and slope in southwestern Oregon, U.S.A.: Society for Economic Paleontolgists and Mineralogists Special Publication No. 27, p. 327-342.

Dunkerley, D. L., 1976, A study of long-term slope stability in the Sydney Basin, Australia: Engineering Geology, v. 10, p. 1-12.

Dunne, T., and Leopold, L. B., 1978, *Water in Environmental Planning*, New York, W. H. Freeman & Co., 818 p.

Fernandes, N. F., and Dietrich, W, E., 1997, Hillslope evolution by diffusive processes: The timescale for equilibrium adjustments: Water Resources Research, v. 33, p. 1307-1318.

Francis, S. C., 1987, Slope development through the threshold slope concept, *in* Anderson, M. G., and Richards, K. S., editors, Slope Stability, Chichester, John Wiley & Sons, p. 601-624.

Freeze, R. A., 1987, Modelling interrelationships between climate, hydrology, and hydrogeology and the development of slopes, *in* Anderson, M. G., and Richards, K. S., editors, Slope Stability, Chichester, John Wiley & Sons, p. 381-403.

Gerstel, W. J., 1999, Deep-Seated Landslide Inventory of th West-Central Olympic Peninsula: Washington Division of Geology and Earth Resources, Open File Report 99-2, 36 p.

Gilbert, G. K., 1877, Geology of the Henry Mountains, U. S. Geographical and Geological Survey of the Rocky Mountain Region: Washington D.C., U.S. Government Printing Office, 160 p.

——— 1909, The convexity of hilltops: Journal of Geology, v. 17, p. 344-350.

Hack, J. T., 1960, Interpretation of erosional topography in humid temperate regions: American Journal of Science, v. 258-A, p. 80-97.

Howard, A. D., 1994, A detachment-limited model of drainage basin evolution: Water Resources Research, v. 30, p. 2261-2285.
Howard, A. D., Dietrich, W. E., and Seidl, M. A., 1994, Modeling fluvial erosion on regional to continental scales: Journal of Geophysical Research, v. 99 p. 13,971-13,986.
Kelsey, H. M., Engebretson, D. C., Mitchell, C. E., and Ticknor, R. L., 1994, Topographic form of the Coast Ranges of the Cascadia Margin in relation to coastal uplift rates and plate subduction: Journal of Geophysical Research, v. 99, p. 12,245-12,255.
Kirkby, M. J., 1971, Hillslope process-response models based on the continuity equation, *in* Brunsden, D., editor, Slopes: Form and Process, Institute of British Geographers Special Publication 3, p. 15-30.
——— 1997, Tectonics in geomorphological models, in Stoddart, D. R., editor, Process and Form in Geomorphology, London, Routledge, p. 121-144.
Koons, P. O., 1995, Modelling the topographic evolution of collisional mountain belts: Review of Earth and Planetary Sciences, v. 23, p. 375-408.
Leopold, L. B., and Maddock, T., 1953, The hydraulic geometry of streams and some physiographic implications: U.S. Geological Survey Professional Paper 252.
Mackin, J. H., 1948, Concept of the graded river: Bulletin of the Geological Society of America, v. 59, p. 463-512.
McNeill, L. C., Goldfinger, C., Kulm, L. D., and Yeats, R. S., 2000, Tectonics of the Neogene Cascadia forearc basin: Investigations of a deformed late Miocene unconformity: Geological Society of America Bulletin, v. 112, p. 1209-1224.
Moglen, G. E., and Bras, R. L., 1995, The effect of spatial heterogeneities on geomorphic expression in a model of basin evolution: Water Resources Research, v. 31, p. 2613-2623.
Montgomery, D. R., 1994, Valley incision and the uplift of mountain peaks: Journal of Geophysical Research, v. 99 p. 13,913-13,921.
Montgomery, D. R., and Buffington, J. M., 1997, Channel reach morphology in mountain drainage basins: Geological Society of America Bulletin, v. 109, p. 596-611.
Montgomery, D. R., and Dietrich, W. E., 1988, Where do channels begin?: Nature, v. 336, p. 232-234.
——— 1992, Channel initiation and the problem of landscape scale: Science, v. 255, p. 826-830.
——— 1994, A physically-based model for the topographic control on shallow landsliding: Water Resources Research, v. 30, p. 1153-1171.
Montgomery, D. R., and Foufoula-Georgiou, E., 1993, Channel network source representation using digital elevation models: Water Resources Research, v. 29, 3925-3934.
Montgomery, D. R., and Greenberg, H., 2000, Local relief and the height of mount Olympus: Earth Surface Processes and Landforms, v. 25, p. 386-396.
Montgomery, D. R., Schmidt, K. M., Greenberg, H., and Dietrich, W. E., 2000, Forest clearing and regional landsliding: Geology, v. 28, p. 311-314.
Montgomery, D. R., Sullivan, K., and Greenberg, H., 1998, Regional test of a model for shallow landsliding: Hydrological Processes, v. 12, p. 943-955.
Moon, B. P., 1984, Refinement of a technique for determing rock mass strength for geomorphological purposes: Earth Surface Processes and Landforms, v. 9, p. 189-193.
Norris, R.J., and Cooper, A.F., 1997, Erosional control on the structural evolution of a transpressional thrust complex on the Alpine Fault, New Zealand: Journal of Structural Geology, v. 19, p. 1323-1342.
O'Loughlin, E.M., 1986, Prediction of surface saturation zones in natural catchments by topographic analysis: Water Resources Research, v. 22, p. 794-804.
Pavlis, T.L., Hamburger, M.W., and Pavlis, G.L., 1997, Erosional processes as a control on the structural evolution of an actively deforming fold and thrust belt: An example from the Pamir-Tien Shan region, central Asia: Tectonics, v. 16, p. 810-822.
Pazzaglia, F. J., and Brandon, M. T., 2001, A fluvial record of long-term steady-state uplift and erosion across the Cascadia forearc high, western Washington State: American Journal of Science, v. 301, p. 385-431.
Penck, W., 1924, Die Morphologische Analyse: Ein Kapital der Physikalischen Geologie, Geographische Abhhandlungen, 2 Reihe, Heft 2, Stuttgart, Engelhorn.
——— 1953, Morphological Analysis of Land Forms: A Contribution to Physical Geology, translated by Czech, H., and Boswell, K. C., London, Macmillian and Co., 429 p.
Personius, S. F., 1995, Late Quaternary stream incision and uplift in the forearc of the Cascadia subduction zone, western Oregon: Journal of Geophysical Research, v. 100, p. 20,193-20,210.
Reneau, S. L., and Dietrich, W. E., 1991, Erosion rates in the southern Oregon Coast Range: Evidence for an equilibrium between hillslope erosion and sediment yield: Earth Surface Processes and Landforms, v. 16, p. 307-322.
Roering, J. J., Kirchner, J. W., and Dietrich, W. E., 1999, Evidence for nonlinear, diffusive sediment transport on hillslopes and implications for landscape morphology: Water Resources Research, v. 35, p. 853-870.
Rouse, W. C., 1975, Engineering properties and slope form in granular soils: Engineering Geology, v. 9, p. 221-235.
Rouse, W. C., and Farhan, Y. I., 1976, Threshold slopes in South Wales: Quarterly Journal of Engineering Geology, v. 9, p. 327-338.
Schmidt, K. M., ms, 1994, Mountain Scale Strength Properties, Deep-Seated Landsliding, and Relief Limits: M.S. thesis, Department of Geological Sciences, University of Washington, Seattle, 166 p.
Schmidt, K. M., and Montgomery, D. R., Limits to relief: Science, v. 270, p. 617-620.
Seidl, M. A., and Dietrich, W. E., 1992, The problem of channel erosion into bedrock, *in* Schmidt, K.-H., and de Ploey, J., Functional Geomorphology, Catena Supplement 23, Cremlingen-Destedt, Catena-Verlag, p. 101-124.
Selby, M. J., 1980, A rock mass strength classification for geomorphic purposes: with tests from Antarctica and New Zealand: Zeitschrift für Geomorpholgie, v. 24, p. 31-51.

——— 1982, Controls on the stability and inclinations of hillslopes formed on hard rock: Earth Surface Processes and Landforms, v. 7, p. 449-467.
——— 1987, Rock slopes, *in* Anderson, M. G., and Richards, K. S., Slope Stability, Chichester, John Wiley & Sons, p. 475-504.
Skempton, A. W., 1964, The long-term stability of clay slopes: Geotechnique, v. 14, p. 75-102.
Snyder, N. P., Whipple, K. X. Tucker, G. E., and Merritts, D. J., 2000, Landscape response to tectonic forcing: Digital elevation model analysis of stream profiles in the Mendocino triple junction region, northern California: Geological Society of America Bulletin, v. 112, p. 1250-1263.
Strahler, A. N., 1950, Equilibrium theory of erosional slopes approached by frequency distribution analysis: American Journal of Science, v. 248, p. 673-696; 800-814.
——— 1956, Quantitative slope analysis: Bulletin of the Geological Society of America, v. 67, p. 571-596.
Stock, J.D., and Montgomery, D. R., 1999, Geologic constraints on bedrock river incision using the stream power law: Journal of Geophysical Research, v. 104, p. 4983-4993.
Tabor, R. W., 1971, Origin of ridge-top depressions by large-scale creep in the Olympic Mountains, Washington: Geological Society of America Bulletin, v. 82, p. 1811-1822.
Tabor, R. W., and Cady, W. M., 1978, The structure of the Olympic Mountains, Washington - Analysis of a subduction zone: U.S. Geological Survey Professional Paper 1033, 38p.
Tarboton, D. G., Bras, R. L., and Rodriguez-Iturbe, I., 1989, Scaling and elevation in river networks: Water Resources Research, v. 25, p. 2037-2051.
——— 1992, A physical basis for drainage density: Geomorphology, v. 5, p. 59-76.
Tucker, G. E., and Slingerland, R. L., 1994, Erosional dynamics, flexural isostasy, and long-lived escarpments: A numerical modeling study: Journal of Geophysical Research, v. 99 p. 12,229-12,243.
Van Asch, Th. W. J., 1983, The stability of slopes in the Ardennes region: Geologie en Mijnbouw, v. 62, p. 683-688.
Whipple, K. X, Kirby, E., and Brocklehurst, S. H., 1999, Geomorphic limits to climate-induced increases in topographic relief: Nature, v. 401, p. 39-43.
Whipple, K. X, and Tucker, G. E., 1999, Dynamics of the stream-power river incision model: implications for height limits of mountain ranges, landscape response timescales, andresearch needs: Journal of Geophysical Research, v. 104, p. 17,661-17,674.
Willett, S., Beaumont, C., and Fullsack, P., 1993, Mechanical model for the tectonics of doubly vergent compressional orogens: Geology, v. 21, p. 371-374.
Willgoose, G., 1994, A physical explanation for an observed area-slope-elevation relationship for catchments with declining relief: Water Resources Research, v. 30, p. 151-159.
Worona, M. A., and Whitlock, C., 1995, Late Quaternary vegetation and climate history near Little Lake, central Coast Range, Oregon: Geological Society of America Bulletin, v. 107, p. 867-876.
Young, A., 1961, Characteristic and limiting slope angles: Zeitschrift für Geomorphologie, v. 5, p. 126-131.
Zeitler, P. K., Chamberlain, C. P., and Smith, H. A., 1993, Synchronous anatexis, metamorphism, and rapid denudation at Nanga Parbat (Pakistan Himalaya): Geology, v. 21, p. 347-350.